



Published in final edited form as:

Biochemistry. 2012 April 3; 51(13): 2950–2957. doi:10.1021/bi300230h.

## Role of Gly117 in the cation/melibiose symport of MelB of *Salmonella typhimurium*

Lan Guan<sup>\*</sup>, S. Vivek Jakkula, Alexey A. Hodkoff, and Yue Su

Department of Cell Physiology & Molecular Biophysics, Center for Membrane Protein Research  
Texas Tech University Health Sciences Center, Lubbock, Texas, 79430

### Abstract

The melibiose permease of *Salmonella typhimurium* (MelB<sub>St</sub>) catalyzes symport of melibiose with Na<sup>+</sup>, Li<sup>+</sup> or H<sup>+</sup>, and bioinformatics analysis indicates that a conserved Gly117 (helix IV) is part of the Na<sup>+</sup>-binding site. We mutated Gly117 to Ala, Pro, Trp or Arg; the effects on melibiose transport and binding of cosubstrates depended on the physical-chemical properties of the side chain. Compared with WT MelB<sub>St</sub>, the Gly117→Ala mutant exhibited little difference in either cosubstrate binding or stimulation of melibiose transport by Na<sup>+</sup> or Li<sup>+</sup>, but all other mutations reduced melibiose active transport and efflux, and decreased the apparent affinity for Na<sup>+</sup>. The bulky Trp at position 117 caused the greatest inhibition of melibiose binding, and Gly117→Arg yielded less than a 4-fold decrease in the apparent affinity for melibiose at saturating Na<sup>+</sup> or Li<sup>+</sup> concentration. Remarkably, the mutant Gly117→Arg catalyzed melibiose exchange in the presence of Na<sup>+</sup> or Li<sup>+</sup>, but did not catalyze melibiose translocation involving net flux of the coupling cation, indicating that sugar is released prior to release of the coupling cation. Taken together, the findings are consistent with the notion that Gly117 plays an important role in cation binding and translocation.

### Keywords

Na<sup>+</sup>-coupled transporter; alternating access; ligand binding; ordered-binding model; Na<sup>+</sup> binding

The melibiose permease of *Salmonella typhimurium* (MelB<sub>St</sub>) catalyzes cotransport of galactoside with Na<sup>+</sup>, Li<sup>+</sup> or H<sup>+</sup>.<sup>1</sup> MelB<sub>St</sub> belongs to the glycoside/pentoside/hexuronide:cation family<sup>2</sup>, a subgroup of the major facilitator superfamily (MFS) of membrane transport proteins. MelB of *Escherichia coli* (MelB<sub>Ec</sub>) is the best-studied member among all MelB orthologues.<sup>3–14</sup> Recently, MelB homologues in human and mouse (called the major facilitator superfamily domain-containing proteins, MFSD) have been reported.<sup>15–17</sup> Among them, MFSD2A protein, which is expressed in many cells, plays a role in adaptive thermogenesis;<sup>15</sup> it has been also identified as a human lung tumor suppressor<sup>16</sup> and responsible for tunicamycin sensitivity in mammalian cells.<sup>17</sup> MFSD2A shares ~15% identity and ~54% similarity of primary sequence with MelB<sub>St</sub>, and the positions essential or important for melibiose transport in MelB are functionally conserved in MFSD2A.<sup>17</sup>

<sup>\*</sup>Corresponding Author: Lan Guan, 3601 4th Street, 5A163, STOP 6551, Lubbock, Texas 79430. Telephone: (806) 743-3102; Fax: (806) 743-1512; and Lan.Guan@ttuhsc.edu.

**SUPPORTING INFORMATION** Conservation between MelB<sub>St</sub> and MelB<sub>Ec</sub>, SDS-PAGE analysis and western blotting, as well as melibiose exchange with intact cells are available free of charge via the Internet at <http://pubs.acs.org>.

The authors declare no competing financial interest.

MelB utilizes the free energy from the downhill translocation of one cosubstrate to drive uphill translocation of the other,<sup>18–22</sup> and all three cations compete for a common binding pocket.<sup>23–25</sup> A previous threading model,<sup>13</sup> basing on the crystal structures of a MFS permease, the H<sup>+</sup>-coupled lactose permease (LacY),<sup>26–28</sup> predicts that MelB<sub>Ec</sub> is organized into two pseudo-symmetrical six-helix bundles connected by a long middle loop surrounding an internal cavity facing the cytoplasm. A similar overall fold for other MelB orthologues has also been proposed from threading analysis.<sup>13</sup> In contrast to LacY, the residues important for cation binding in MelB are located in the N-terminal helix bundle (Fig. 1), whereas the H<sup>+</sup>-binding site in LacY is located primarily in the C-terminal helices.<sup>28</sup> Based on the location of the sugar-binding site in LacY, the melibiose-binding site is proposed to lie within the internal cavity (Fig. 1).<sup>13</sup> This model is consistent with numerous biochemical and biophysical results,<sup>11, 29–36</sup> as well as low-resolution EM structures of MelB<sub>Ec</sub>.<sup>37, 38</sup> The organization of the protein into two separate helix bundles, as well as the location of cosubstrates, are consistent with the alternating-access transport model, which has been recognized as a fundamental mechanism for many other secondary transporters.<sup>26, 39–46</sup>

MelB<sub>St</sub> shares 86% identity and 96% similarity of primary sequence with MelB<sub>Ec</sub> (Supplemental Information, Fig. S1). All non-conserved and 82% of the conserved variations occur in the C-terminal domain and the middle loop. Bioinformatics analysis suggests that the internal cavities including two cosubstrate-binding sites are well conserved between the two MelB permeases (Fig. 1), implying similarity in function, which is supported by previous studies of melibiose transport and cation binding.<sup>1</sup> The docked sugar is surrounded by potential H-bonding partners and aromatic residues (Fig. 1),<sup>13</sup> which share common features for sugar binding.<sup>41, 47–50</sup> A Na<sup>+</sup> has been proposed to bind between helices II and IV<sup>13</sup>. A large body of experimental data, including those from mutagenesis, biochemistry and FTIR spectroscopy, indicates that the carboxyl groups of conserved Asp55 and Asp59 (helix II) contribute to Na<sup>+</sup> binding to MelB<sub>Ec</sub>.<sup>14, 29–34</sup> Helix IV is in the center of a charge/H-bond network involved in the binding of the two cosubstrates (Fig. 1).<sup>13, 30, 34, 51</sup> Gly117 is in the middle of helix IV, and the carbonyl oxygen may participate in Na<sup>+</sup> coordination (Fig. 1).<sup>13</sup>

We know little about the role of Gly117, but it was observed that the G117D mutation rescued the function of inactive mutant D55S in MelB<sub>Ec</sub>,<sup>52</sup> which supports the notion that Gly117 is in close proximity to Asp55.<sup>13, 52</sup> In addition, in mutant G117C MelB<sub>Ec</sub> the conformational equilibrium was displaced towards the outward-facing conformation.<sup>53</sup> In MelB<sub>St</sub>, site-directed mutagenesis has not been used to study the binding sites for cosubstrates so far. In this study, we mutated Gly117 of MelB<sub>St</sub> to four different residues--Ala, Pro, Trp or Arg. The effects of the mutations on cosubstrate binding and transport depend on the physical and chemical properties of the side chain. Our studies indicate that Gly117 plays an important role in cation binding and translocation, which is consistent with our threading model.

## Materials and Methods

### Materials

[1-<sup>3</sup>H]Melibiose was custom synthesized by PerkinElmer (Boston, MT). The 2'-(N-dansyl)aminoalkyl-1-thio-β-D-galactopyranoside (D<sup>2</sup>G) was kindly provided by Drs. H. Ronald Kaback and Gérard Leblanc. Monensin and carbonyl cyanide m-chlorophenylhydrazone (CCCP) were purchased from *Sigma-Aldrich*. 2-(4'-maleimidylanilino)-naphthalene-6-sulfonic acid was purchased from *Invitrogen*. Oligodeoxynucleotides were synthesized by *Integrated DNA Technologies*. MacConkey agar media (lactose free) was from *Difco*. All other materials were reagent grade and obtained from commercial sources.

## Bacterial strains and plasmids

*E. coli* DW2 strain (*melA*<sup>+</sup>,  $\Delta$ *melB*,  $\Delta$ *lacZY*), obtained from Dr. Gérard Leblanc, was used for the functional characterization. *E. coli* XL1 Blue cells were used for DNA manipulations. The expression plasmid pK95  $\Delta$ AH/MelB<sub>S<sub>t</sub></sub>/CHis<sub>10</sub>,<sup>1, 3</sup> which encodes the full length MelB<sub>S<sub>t</sub></sub> with L5→M and a His<sub>10</sub>-tag at the C-terminus (the wild type) was used as the template. Four individual mutants with residue Ala, Pro, Trp or Arg at position Gly117 were constructed by *QuickChange*<sup>™</sup> *Site-Directed Mutagenesis Kit* from *Stratagene*. All mutants have been confirmed by DNA sequencing.

## Growth of cells and protein overexpression

*E. coli* DW2 cells (*melA*<sup>+</sup>, *melB*, *lacZY*) containing a given plasmid were grown in Luria-Bertani (LB) broth with 100 mg/L of ampicillin in a 37-°C shaker overnight. The overnight cultures were diluted by 5% to LB broth supplemented with 0.5% glycerol and 100 mg/L of ampicillin, and constitutive overexpression was obtained by shaking at 30 °C for 5 h.

## Preparation of right-side-out (RSO) membrane vesicles

RSO membrane vesicles were prepared from *E. coli* DW2 cells by osmotic lysis,<sup>1, 54, 55</sup> extensively washed and resuspended in 100 mM KP<sub>i</sub> (pH 7.5) at a protein concentration of ~25–30 mg/ml, frozen in liquid N<sub>2</sub>, and stored at –80 °C.

## Preparation of crude membranes

The 5-hour cultures with the expressed MelB<sub>S<sub>t</sub></sub> were washed with 20 mM Tris-HCl (pH 7.5) once, re-suspended and adjusted with the same buffer to A<sub>600</sub> ~20. Approximately 100  $\mu$ L of cells from each sample were sonicated in an ice-cold water bath (Branson 2510) for 5 min, three times; and centrifuged at 20,816 g for 15 min at 4 °C. The supernatant (80  $\mu$ L) was subjected to ultracentrifugation at 384,492 g (TLA-100 rotor, *Beckman Optima*<sup>™</sup> Max Ultracentrifuge) for 20 min; the pellets were resuspended in 70  $\mu$ L of 20 mM Tris-HCl (pH 7.5).

## SDS-12% PAGE and Western blotting

After protein assay using *Micro BCA*<sup>™</sup> *Protein Assay Kit* (Pierce), ~15 g of total membranes were loaded onto each well of SDS-12%PAGE. The gel was transferred onto the PVDF membrane by the *Trans-Blot Turbo* transfer system (*Bio-Rad*) at 1.3 A, 25 V for 15 min. The blocked PVDF membrane was then reacted with the penta-His horseradish peroxidase conjugate and washed according to the protocols provided in the *Penta-His HRP Conjugate Kit* (*Qiagen*). MelB<sub>S<sub>t</sub></sub> proteins were detected using the *SuperSignal West Pico* chemiluminescent substrate (*Thermo Scientific*) after exposing it to the X-ray film (*Kodak BioMax XAR film*).

## [1-<sup>3</sup>H]Melibiose transport assay

*E. coli* DW2 cells expressing MelB<sub>S<sub>t</sub></sub> in the absence of melibiose were washed with 50 ml of 100 mM KP<sub>i</sub> (pH 7.5, so-called Na<sup>+</sup>-free buffer) twice, followed by washing with 50 ml 100 mM KP<sub>i</sub>, pH 7.5, 10 mM MgSO<sub>4</sub>. The cell pellets were resuspended with the latter buffer, adjusted to an A<sub>420</sub> = 10 (~0.7 mg protein/ml). Melibiose transport at a final concentration of 0.4 mM and a specific activity of 10 mCi/mmol was assayed as described.<sup>1</sup>

## Melibiose fermentation

The DW2 cells (*melA*<sup>+</sup>,  $\Delta$ *melB*,  $\Delta$ *lacZY*) were transformed with a given plasmid, plated on MacConkey agar plates<sup>35</sup> containing ~100 mM Na<sup>+</sup> with supplement of 1–30 mM melibiose

(the sole carbohydrate source) and 100 mg/L of ampicillin, and incubated at 37 °C. After 18 h, the plates were viewed and photographed immediately.

### Melibiose efflux and exchange

RSO membrane vesicles containing MelB<sub>St</sub> in 100 mM KP<sub>i</sub>, pH 7.5, 10 mM MgSO<sub>4</sub> were concentrated to 25–30 mg/ml, and pre-equilibrated overnight on ice with melibiose (20 mM, 10 mCi/mmol), 0.75 μM monensin, and 10 μM CCCP<sup>22</sup>, in the absence or presence 20 mM NaCl or LiCl. Aliquots (2 μL) were diluted 200 fold into a given buffer in the absence (efflux) or presence (exchange) of 20 mM unlabeled melibiose, and reactions were terminated by dilution and rapid filtration at a given time.<sup>1</sup>

### FRET (Trp→D<sup>2</sup>G)

Fluorescence was measured with an AMINCO-Bowman Series 2 Spectrometer. Steady-state measurements were performed in a 3-mm quartz cuvette (*Starna Cells, Inc*) with RSO membrane vesicles at a protein concentration of ~0.5 mg/ml in 100 mM KP<sub>i</sub>, pH 7.5. With excitation wavelength at 290 nm, the FRET intensity was recorded for 60 sec at 500 nm with slit widths of 2 mm for both excitation and emission.

### Determination of apparent cation-stimulation constants ( $K_{0.5}^{Na+}$ and $K_{0.5}^{Li+}$ ) of the D<sup>2</sup>G FRET

NaCl or LiCl was consecutively added into a 3-mm quartz cuvette containing RSO vesicles after an addition of 10 μM D<sup>2</sup>G (a  $K_D$  value for the WT). Water at identical volume was used for the control. The FRET signals were recorded for 60 sec at each condition and mean values were used for further calculation. The increase in intensity ( $\Delta I^{Na+ \text{ or } Li+}$ ), the difference before ( $I_0$ ) and after successive additions of cation solution ( $I^{Na+ \text{ or } Li+}$ ), was expressed as the percentage of the  $I_0$  ( $\Delta I^{Na+ \text{ or } Li+}/I_0$ ). FRET stimulation at each cation concentration was corrected by subtracting corresponding  $I^{water}/I_0$  value, and then plotted as a function of Na<sup>+</sup> or Li<sup>+</sup> concentration. The  $K_{0.5}^{Na+ \text{ or } Li+}$  values are determined by fitting the data to a hyperbolic function.

### Determination of the melibiose concentration corresponding to half-maximal displacement of bound D<sup>2</sup>G (IC<sub>50</sub>)

Melibiose was added stepwise to a 3-mm quartz cuvette containing RSO vesicles after the additions with D<sup>2</sup>G (10 μM) and NaCl or LiCl (20 mM or 200 mM) until no change occurred in fluorescence emission at 500 nm. An identical volume of water was added at each point as a negative control. FRET signals were recorded for 60 sec after each addition, and mean values were calculated. The decrease in intensity after each addition of melibiose ( $\Delta F^{Mel}$ ) was corrected by subtracting the emission change obtained with water ( $\Delta F^{water}$ ), and plotted as a function of melibiose concentration. The IC<sub>50</sub> values were determined by fitting the data to a hyperbolic function.

## RESULTS

### Construction and protein expression of Gly117 mutants

Gly at position 117 in MelB<sub>St</sub> was changed by site-directed mutagenesis to four different residues: Ala (small volume); Pro (a helix destabilizer); Trp (aromatic ring); or Arg (positive charge). Membrane proteins were separated by SDS-PAGE, and the proteins were detected by both silver nitrate and Western blot using anti-His antibody (Supplemental Fig. S2). Compared to the WT, most of the mutants had similar levels of membrane expression, with the exception of G117R, which had a reduced expression.

### Melibiose active transport in intact cells

In a nominally  $\text{Na}^+$ -free buffer, the WT catalyzes melibiose transport at an almost linear rate for 15 s to 80 nmol/mg protein at 2 min (Fig. 2), which was significantly stimulated by  $\text{Na}^+$  or  $\text{Li}^+$  as shown previously.<sup>1, 56</sup> Addition of the protonophore CCCP abolished transport, indicating that the primary driving force for transport is the electrochemical  $\text{H}^+$  gradient. Furthermore, when unlabeled melibiose was added at each time point during transport, with a 10-min incubation prior to the filtration, the entire internal pool of melibiose was exchanged with extracellular melibiose (Supplemental Information, Fig. S3). Thus, there is little or no hydrolysis or chemical alteration of the accumulated intracellular melibiose.

The mutant G117A catalyzed  $\text{Na}^+$ - or  $\text{Li}^+$ -dependent melibiose transport similar to the WT (Fig. 2) with somewhat lower  $\text{H}^+$ -coupled transport activity (i.e., in the absence of  $\text{Na}^+$  or  $\text{Li}^+$ ). All other mutants (P, W or R) exhibited  $\text{H}^+$ -coupled melibiose transport at a level indistinguishable from CCCP-treated WT or non-transformed DW2 cells, and showed no response to addition of  $\text{Na}^+$  or  $\text{Li}^+$ .

### Melibiose fermentation

On MacConkey agar plates containing 1–30 mM melibiose, untransformed DW-2 cells formed pale/white colonies with a translucent background, denoting little or no melibiose translocation across the membranes. At >10 mM melibiose, DW2 cells, containing the chromosome-encoded  $\alpha$ -galactosidase and recombinantly overexpressing WT MelB<sub>St</sub>, formed magenta colonies on a hazy background indicating melibiose fermentation and therefore downhill melibiose influx catalyzed by MelB<sub>St</sub> (Fig. 3). At 5 mM melibiose, few colonies were pink, whereas at 2.5 mM or lower, the colonies were pale yellow/brown. Mutant G117A exhibited similar color to WT. Mutant G117P exhibited red or pink colonies only at high concentrations of melibiose, indicating limited melibiose influx and fermentation. Mutants G117R and G117W formed colonies that were indistinguishable from untransformed cells even at 30 mM melibiose, indicating no fermentation.

### Melibiose efflux and exchange

In the absence of  $\text{Na}^+$  or  $\text{Li}^+$ , RSO membrane vesicles containing WT MelB<sub>St</sub> exhibited a slow rate of melibiose efflux down a concentration gradient and a slightly faster rate of equilibrium exchange (Fig. 4). Whereas the efflux rate was stimulated by  $\text{Na}^+$  or  $\text{Li}^+$ , the exchange rate was enhanced by  $\text{Na}^+$  but inhibited by  $\text{Li}^+$ .<sup>1</sup> In the presence of  $\text{Na}^+$ , 96% of the intravesicular melibiose exchanged with the extracellular unlabeled melibiose within 5 min (data not shown). Consistent with the results in intact cells, little or no melibiose hydrolysis occurred within the RSO vesicles.

The G117W mutant did not catalyze either melibiose efflux or exchange in the presence of  $\text{H}^+$ ,  $\text{Na}^+$  or  $\text{Li}^+$ . The G117P mutant catalyzed significantly reduced rates of efflux and exchange. Strikingly, mutant G117R exhibited little or no efflux but catalyzed a relatively fast rate of exchange in the presence of  $\text{Na}^+$  or  $\text{Li}^+$ , but not  $\text{H}^+$ .

### $K_{0.5}^{\text{Na}^+}$ or $K_{0.5}^{\text{Li}^+}$ for D<sup>2</sup>G FRET

FRET from endogenous Trp residues to the dansyl moiety of bound D<sup>2</sup>G has been demonstrated with MelB<sub>Ec</sub><sup>4, 57</sup> and MelB<sub>St</sub>.<sup>1</sup> Thus, WT MelB<sub>St</sub> exhibits FRET upon the addition of D<sup>2</sup>G, which is stimulated by addition of  $\text{Na}^+$  or  $\text{Li}^+$  and reversed by melibiose. The difference in intensity observed before and after melibiose addition reflects the D<sup>2</sup>G bound specifically to MelB<sub>St</sub>. At saturating  $\text{Na}^+$  or  $\text{Li}^+$ , the WT MelB<sub>St</sub> exhibits  $K_d$  for D<sup>2</sup>G of ~10  $\mu\text{M}$ .<sup>1</sup> The  $\text{Na}^+$  or  $\text{Li}^+$  enhancement of FRET (difference in intensity before and after cation addition,  $\Delta I^{\text{Na}^+ \text{ or } \text{Li}^+}$ ) results from combined effects of an increase of D<sup>2</sup>G binding *per se* and a conformational change (distance and/or environment) induced by  $\text{Na}^+$  or  $\text{Li}^+$



binding.<sup>1, 4</sup> Mutations may affect Na<sup>+</sup>- or Li<sup>+</sup>-induced intensities by (a) decreasing the binding affinity for either or both cosubstrates, and/or (b) modifying the micro-environment surrounding donor Trp residue(s), and/or (c) restricting the conformational change. Thus, the same concentrations of Na<sup>+</sup>- or Li<sup>+</sup>-bound ternary complex from different mutants may not yield the same  $\Delta I/I_0$  value.

In order to quantify cation binding to MelB<sub>St</sub> mutants,  $\Delta I^{\text{Na}^+ \text{ or Li}^+}/I_0$  was measured as a function of Na<sup>+</sup> or Li<sup>+</sup> concentration (Fig. 5, upper panels). The stimulation constants ( $K_{0.5}^{\text{Na}^+}$  and  $K_{0.5}^{\text{Li}^+}$ ) for D<sup>2</sup>G FRET in WT MelB<sub>St</sub> were 0.9 mM and 1.5 mM, respectively, and the mutant G117A yielded similar values (Table 1).  $K_{0.5}^{\text{Na}^+}$  and  $K_{0.5}^{\text{Li}^+}$  values for G117P were 25- and 6-fold higher than those for the WT, respectively. With mutant G117R, both  $K_{0.5}$  values increased by 12 fold. The  $K_{0.5}^{\text{Li}^+}$  for G117W was only 2.5-fold higher than obtained for WT, but no Na<sup>+</sup> stimulation was observed even at 500 mM (data not shown). In all three mutants, the maximum stimulations by Na<sup>+</sup> or Li<sup>+</sup> were largely reduced implying that either the micro-environment and/or distance between D<sup>2</sup>G and donors are changed, or that the number of bound D<sup>2</sup>G molecules is reduced by lower sugar affinity. In either case, the constant ( $K_{0.5}^{\text{Na}^+ \text{ or Li}^+}$ ) reflects the cation-binding affinity.

### IC<sub>50</sub> for melibiose displacement of bound D<sup>2</sup>G

In order to quantify melibiose binding to MelB<sub>St</sub>, 10  $\mu$ M D<sup>2</sup>G, Na<sup>+</sup> or Li<sup>+</sup>, and then the titrate melibiose were consecutively added to RSO vesicles. IC<sub>50</sub> values for WT MelB<sub>St</sub> of 3.8 mM or 1.7 mM were observed at 20 mM Na<sup>+</sup> or Li<sup>+</sup>, respectively, and 2.2 mM or 1.8 mM at 200 mM Na<sup>+</sup> or Li<sup>+</sup>, respectively (Fig. 5, bottom panels; Table 2). The IC<sub>50</sub> for mutant G117A was about 2-fold higher than that of the WT at 20 mM Na<sup>+</sup> or Li<sup>+</sup>. In the presence of 20 mM or 200 mM of Li<sup>+</sup>, IC<sub>50</sub> values for mutant G117W were 50 mM or 14.1 mM, respectively, and for mutant G117P were 11.3 mM or 7.5 mM, respectively. Mutant G117R exhibited IC<sub>50</sub> of 5.6 mM or 4.7 mM in the presence of 200 mM Na<sup>+</sup> or Li<sup>+</sup>. FRET intensities for mutants G117W or P, with Na<sup>+</sup> as the cosubstrate, were too weak to allow the determination of IC<sub>50</sub> value.

## DISCUSSION

An ordered-binding model for cation/melibiose symport in MelB<sub>Ec</sub> has been suggested.<sup>11, 13, 14</sup> An extended model for the melibiose efflux mechanism is proposed for MelB<sub>St</sub> here (Fig. 6). In this simplified scheme, melibiose efflux down a sugar concentration gradient consists of 8 steps (*black solid arrows*): [*Step-1, Na<sup>+</sup>-bound inward-facing state, or P<sub>i</sub>:Na<sup>+</sup> state*] Binding of a Na<sup>+</sup> to the inward-facing conformer; [*Step-2, Na<sup>+</sup>- and melibiose-bound inward-facing state, or P<sub>i</sub>:Na<sup>+</sup>:Mel state*] Binding of a melibiose from the cytoplasmic cavity; [*Step-3, occluded Na<sup>+</sup>- and melibiose-bound state, or P:(Na<sup>+</sup>:Mel) state*] Formation of a ternary-complex intermediate that is occluded on both sides; [*Step-4, Na<sup>+</sup>- and melibiose-bound outward-facing state, or P<sub>o</sub>:Na<sup>+</sup>:Mel state*] Opening of the periplasmic cavity; [*Step-5, Na<sup>+</sup>-bound outward-facing state, or P<sub>o</sub>:Na<sup>+</sup> state*] Release of the melibiose at the outer surface; [*Step-6, empty outward-facing state, or P<sub>o</sub>:empty state*] Release of Na<sup>+</sup> from an outward-facing conformer; [*Step-7, occluded empty state, or P:(empty) state*] Formation of an unloaded intermediate occluded on both sides; [*Step-8, empty inward-facing state, or P<sub>i</sub>:empty state*] Opening of the cytoplasmic cavity. The melibiose efflux involves the whole cycle, and melibiose exchange reaction involves only steps 1–5.

Previously, we have experimentally determined<sup>1</sup> that the extracellular release of cation is the rate-limiting step for melibiose efflux catalyzed by MelB<sub>St</sub>, and melibiose is released from MelB<sub>St</sub> extracellularly prior to the release of Na<sup>+</sup>. These results are consistent with what observed in MelB<sub>Ec</sub>.<sup>22</sup> Here, we provide further evidence to support this notion. Cells expressing mutant G117R neither ferment melibiose nor catalyze melibiose active transport

or efflux. Remarkably, however, this mutant catalyzes Na<sup>+</sup>- or Li<sup>+</sup>- but not H<sup>+</sup>-coupled equilibrium exchange. Thus, in the presence of 20 mM melibiose and Na<sup>+</sup> or Li<sup>+</sup> on both sides of the membrane, the mutant can undergo the global conformational change involved in an alternating access-type mechanism but is defective in releasing Na<sup>+</sup> or Li<sup>+</sup> (Fig. 6, *step 6*), implying that Gly117 plays an important role in the cation translocation mechanism. This behavior of mutant G117R, similar to that of E325A LacY<sup>58; 59</sup>, strongly supports the ordered-binding mechanism as postulated (Fig. 6).

The rate of exchange is believed to correlate with the binding affinity. Accordingly, at saturating Na<sup>+</sup> or Li<sup>+</sup> concentration, the IC<sub>50</sub> for melibiose displacement of bound D<sup>2</sup>G exhibits only a 2.5-fold increase (Table 2). If we assume that the mutation has a similar effect on D<sup>2</sup>G and melibiose, then it can be estimated that the apparent binding constant ( $K_d$ ) for melibiose is increased by less than 4 fold, implying that sugar binding is only slightly affected by the Arg at position 117, and therefore Gly117 may not coordinate melibiose directly.

In WT MelB<sub>St</sub>, we have been observed previously<sup>1</sup> that Li<sup>+</sup> stimulates melibiose efflux and an outwardly directed Li<sup>+</sup> gradient increases exchange; however, at equal Li<sup>+</sup> concentrations on both sides of the membrane, the melibiose exchange rate is slower than the efflux rate. In MelB<sub>Ec</sub>,<sup>22,60</sup> Li<sup>+</sup> also inhibits melibiose exchange, but not methyl-β-D-thiogalactoside exchange. Although the mechanism of inhibition is still not clear, it is possible that MelB/Li<sup>+</sup>/melibiose complexes favor an occluded state (Fig. 6, *step 3*) in which there is no exchange between free and bound sugars.<sup>1</sup> In the presence of Li<sup>+</sup>, the Gly117→R mutation inhibits melibiose efflux but stimulates exchange at a rate even faster than that obtained with WT MelB<sub>St</sub>. It is likely that the mutation may decrease the stability of the MelB/Li<sup>+</sup>/melibiose complexes at *step 3*, thus facilitating melibiose exchange at a rate similar to that obtained in the presence of Na<sup>+</sup>.

Six of eight endogenous Trp residues are located in the N-terminal helix bundle. Trp64 (helix II) and Trp299 (IX) of MelB<sub>Ec</sub> are responsible for 80% of the D<sup>2</sup>G FRET, and apparently Trp116 does not contribute significantly to the FRET.<sup>25</sup> Thus, it seems unlikely that the inserted Trp at position 117 could serve as an efficient FRET donor or significantly quench the Trp64 and Trp299 emission directly. Mutant G117W specifically blocked Na<sup>+</sup>-induced D<sup>2</sup>G FRET (ΔI), but the apparent affinity for Li<sup>+</sup> did not change significantly (< 3-fold increase in  $K_{0.5}^{Li^+}$ , Table 1). Thus, lack of Na<sup>+</sup>-induced D<sup>2</sup>G FRET (ΔI) may be mainly due to a large decrease in Na<sup>+</sup> binding.

While in most Gly117 mutants there are reductions in binding of Na<sup>+</sup>, Li<sup>+</sup> and melibiose, the effect on Na<sup>+</sup> binding is more severe than those on Li<sup>+</sup> and melibiose. The MelB orthologue of *Klebsiella pneumoniae* (MelB<sub>Kp</sub>) couples melibiose transport with H<sup>+</sup> and Li<sup>+</sup> but not Na<sup>+</sup>.<sup>61</sup> It has been demonstrated that Asn58, which is adjacent to Asp59, is important for Na<sup>+</sup> recognition, and MelB<sub>Kp</sub> has Ala at position 58.<sup>31</sup> It seems likely that selective elimination of Na<sup>+</sup> binding in MelB could be achieved by a minor modification around the cation-binding site. In addition, the effective inhibition of melibiose binding in mutant G117W (Table 2) may be due to a steric effect of the bulky side chain, which may also partially account for the effects of other mutations on sugar binding.

Gly is known to destabilize α-helices, and the replacement with Pro, another α-helix destabilizer that may alter the tilt in helix IV, partially inhibits both efflux and exchange reactions, as well as impairs affinity for the cosubstrates to a similar extent. Thus, the data support the notion that the melibiose/cation symport mechanism requires precise positioning of helix IV.

If the carbonyl oxygen at position 117 is a part of the cation-binding site, then a small neutral replacement should not have a significant effect. Accordingly, placement of Ala at position 117 has little or no effect on Na<sup>+</sup>- or Li<sup>+</sup>-coupled melibiose transport (Fig. 2) or the apparent affinity for Na<sup>+</sup>, Li<sup>+</sup> or melibiose (Tables 1 & 2). Taken as a whole, our findings show that the placement of Arg or Trp at position 117 abolishes melibiose uphill transport, efflux, and fermentation; G117R and P greatly decrease apparent affinities for Na<sup>+</sup> and Li<sup>+</sup>. Remarkably, the mutant G117R retains significant sugar affinity and catalyzes melibiose exchange, a partial reaction, with bound Na<sup>+</sup> or Li<sup>+</sup>, but does not catalyze melibiose translocation involving net flux of the coupling cation. In conclusion, Gly117 plays an important role in cation binding and translocation of MelB<sub>ST</sub>, which is consistent with our threading structure.<sup>13</sup>

## Supplementary Material

Refer to Web version on PubMed Central for supplementary material.

## Acknowledgments

The authors thank Drs. Gérard Leblanc, Klaus Fendler, Luis Reuss, and H. Ronald Kaback for materials, critical reading, and helpful discussions; Drs. Hariharan Parameswaran and Anowarul Amin for reading of this manuscript; Ms. Shailika Nurva and Dr. Mohammad Yousef for their excellent technical support in the earlier stages of this project. SVJ & YS, Master student interns from Center for Biotechnology and Genomics at Texas Tech University; AAH, undergraduate student at TTU.

This work was supported by Texas Norman Hackerman Advanced Research Program 010674-0034-2009, National Institutes of Health Grants R01 GM095538, and R21HL087895-02S1 to L.G.

## ABBREVIATIONS

<b>MelB<sub>St</sub></b>	melibiose permease of <i>Salmonella typhimurium</i>
<b>MelB<sub>Ec</sub></b>	MelB of <i>Escherichia coli</i>
<b>LacY</b>	lactose permease of <i>E. coli</i>
<b>mela</b>	gene encoding α-galactosidase
<b>LB broth</b>	Luria-Bertani broth
<b>D<sup>2</sup>G</b>	2'-(N-dansyl)aminoalkyl-1-thio-β-D-galactopyranoside
<b>CCCP</b>	carbonylcyanide-m-chlorophenylhydrazone
<b>K<sub>0.5</sub><sup>Na+ or Li+</sup></b>	the Na <sup>+</sup> or Li <sup>+</sup> stimulation constant for D <sup>2</sup> G FRET
<b>IC<sub>50</sub></b>	the melibiose concentration corresponding to half-maximal displacement of bound D <sup>2</sup> G.

## REFERENCES

- (1). Guan L, Nurva S, Ankeshwarapu SP. Mechanism of melibiose/cation symport of the melibiose permease of *Salmonella typhimurium*. *J Biol Chem*. 2011; 286:6367–6374. [PubMed: 21148559]
- (2). Saier MH Jr. Families of transmembrane sugar transport proteins. *Mol Microbiol*. 2000; 35:699–710. [PubMed: 10692148]
- (3). Pourcher T, Leclercq S, Brandolin G, Leblanc G. Melibiose permease of *Escherichia coli*: large scale purification and evidence that H<sup>+</sup>, Na<sup>+</sup>, and Li<sup>+</sup> sugar symport is catalyzed by a single polypeptide. *Biochemistry*. 1995; 34:4412–4420. [PubMed: 7703254]



- (4). Maehrel C, Cordat E, Mus-Veteau I, Leblanc G. Structural studies of the melibiose permease of *Escherichia coli* by fluorescence resonance energy transfer. I. Evidence for ion-induced conformational change. *J Biol Chem.* 1998; 273:33192–33197. [PubMed: 9837887]
- (5). Ganea C, Pourcher T, Leblanc G, Fendler K. Evidence for intraprotein charge transfer during the transport activity of the melibiose permease from *Escherichia coli*. *Biochemistry.* 2001; 40:13744–13752. [PubMed: 11695924]
- (6). Ding PZ, Wilson TH. The effect of modifications of the charged residues in the transmembrane helices on the transport activity of the melibiose carrier of *Escherichia coli*. *Biochem Biophys Res Commun.* 2001; 285:348–354. [PubMed: 11444849]
- (7). Leon X, Lorenz-Fonfria VA, Lemonnier R, Leblanc G, Padros E. Substrate-induced conformational changes of melibiose permease from *Escherichia coli* studied by infrared difference spectroscopy. *Biochemistry.* 2005; 44:3506–3514. [PubMed: 15736960]
- (8). Abdel-Dayem M, Basquin C, Pourcher T, Cordat E, Leblanc G. Cytoplasmic loop connecting helices IV and V of the melibiose permease from *Escherichia coli* is involved in the process of Na<sup>+</sup>-coupled sugar translocation. *J Biol Chem.* 2003; 278:1518–1524. [PubMed: 12421811]
- (9). Leon X, Lemonnier R, Leblanc G, Padros E. Changes in secondary structures and acidic side chains of melibiose permease upon cosubstrates binding. *Biophys J.* 2006; 91:4440–4449. [PubMed: 17012318]
- (10). Garcia-Celma JJ, Dueck B, Stein M, Schlueter M, Meyer-Lipp K, Leblanc G, Fendler K. Rapid activation of the melibiose permease MelB immobilized on a solid-supported membrane. *Langmuir.* 2008; 24:8119–8126. [PubMed: 18572928]
- (11). Meyer-Lipp K, Sery N, Ganea C, Basquin C, Fendler K, Leblanc G. The inner interhelix loop 4–5 of the melibiose permease from *Escherichia coli* takes part in conformational changes after sugar binding. *J Biol Chem.* 2006; 281:25882–25892. [PubMed: 16822867]
- (12). Leon X, Leblanc G, Padros E. Alteration of sugar-induced conformational changes of the melibiose permease by mutating Arg141 in loop 4–5. *Biophys J.* 2009; 96:4877–4886. [PubMed: 19527646]
- (13). Yousef MS, Guan L. A 3D structure model of the melibiose permease of *Escherichia coli* represents a distinctive fold for Na<sup>+</sup> symporters. *Proc Natl Acad Sci U S A.* 2009; 106:15291–15296. [PubMed: 19706416]
- (14). Granell M, Leon X, Leblanc G, Padros E, Lorenz-Fonfria VA. Structural insights into the activation mechanism of melibiose permease by sodium binding. *Proc Natl Acad Sci U S A.* 2010; 107:22078–22083. [PubMed: 21135207]
- (15). Angers M, Uldry M, Kong D, Gimble JM, Jetten AM. Mfsd2a encodes a novel major facilitator superfamily domain-containing protein highly induced in brown adipose tissue during fasting and adaptive thermogenesis. *Biochemical J.* 2008; 416:347–355.
- (16). Spinola M, Falvella FS, Colombo F, Sullivan JP, Shames DS, Girard L, Spessotto P, Minna JD, Dragani TA. MFSD2A is a novel lung tumor suppressor gene modulating cell cycle and matrix attachment. *Molecular Cancer.* 2010; 9:62. [PubMed: 20236515]
- (17). Reiling JH, Clish CB, Carette JE, Varadarajan M, Brummelkamp TR, Sabatini DM. From the Cover: Feature Article: A haploid genetic screen identifies the major facilitator domain containing 2A (MFSD2A) transporter as a key mediator in the response to tunicamycin. *Proc Natl Acad Sci U S A.* 2011; 108:11756–11765. [PubMed: 21677192]
- (18). Wilson DM, Wilson TH. Cation specificity for sugar substrates of the melibiose carrier in *Escherichia coli*. *Biochim Biophys Acta.* 1987; 904:191–200. [PubMed: 3311166]
- (19). Tokuda H, Kaback HR. Sodium-dependent methyl 1-thio-β-d-galactopyranoside transport in membrane vesicles isolated from *Salmonella typhimurium*. *Biochemistry.* 1977; 16:2130–2136. [PubMed: 16639]
- (20). Tokuda H, Kaback HR. Sodium-dependent binding of p-nitrophenyl alpha-d-galactopyranoside to membrane vesicles isolated from *Salmonella typhimurium*. *Biochemistry.* 1978; 17:698–705. [PubMed: 341975]
- (21). Tsuchiya T, Raven J, Wilson TH. Co-transport of Na<sup>+</sup> and methyl-beta-d-thiogalactopyranoside mediated by the melibiose transport system of *Escherichia coli*. *Biochem Biophys Res Commun.* 1977; 76:26–31. [PubMed: 17404]

- (22). Bassilana M, Pourcher T, Leblanc G. Facilitated diffusion properties of melibiose permease in *Escherichia coli* membrane vesicles. Release of co-substrates is rate limiting for permease cycling. *J Biol Chem.* 1987; 262:16865–16870. [PubMed: 3316227]
- (23). Lopilato J, Tsuchiya T, Wilson TH. Role of Na<sup>+</sup> and Li<sup>+</sup> in thiomethylgalactoside transport by the melibiose transport system of *Escherichia coli*. *J Bacteriol.* 1978; 134:147–156. [PubMed: 25882]
- (24). Damiano-Forano E, Bassilana M, Leblanc G. Sugar binding properties of the melibiose permease in *Escherichia coli* membrane vesicles. Effects of Na<sup>+</sup> and H<sup>+</sup> concentrations. *J Biol Chem.* 1986; 261:6893–6899. [PubMed: 3516999]
- (25). Mus-Veteau I, Pourcher T, Leblanc G. Melibiose permease of *Escherichia coli*: substrate-induced conformational changes monitored by tryptophan fluorescence spectroscopy. *Biochemistry.* 1995; 34:6775–6783. [PubMed: 7756309]
- (26). Abramson J, Smirnova I, Kasho V, Verner G, Kaback HR, Iwata S. Structure and mechanism of the lactose permease of *Escherichia coli*. *Science.* 2003; 301:610–615. [PubMed: 12893935]
- (27). Mirza O, Guan L, Verner G, Iwata S, Kaback HR. Structural evidence for induced fit and a mechanism for sugar/H<sup>+</sup> symport in LacY. *EMBO J.* 2006; 25:1177–1183. [PubMed: 16525509]
- (28). Guan L, Mirza O, Verner G, Iwata S, Kaback HR. Structural determination of wild-type lactose permease. *Proc Natl Acad Sci U S A.* 2007; 104:15294–15298. [PubMed: 17881559]
- (29). Pourcher T, Deckert M, Bassilana M, Leblanc G. Melibiose permease of *Escherichia coli*: mutation of aspartic acid 55 in putative helix II abolishes activation of sugar binding by Na<sup>+</sup> ions. *Biochem Biophys Res Commun.* 1991; 178:1176–1181. [PubMed: 1872836]
- (30). Pourcher T, Zani ML, Leblanc G. Mutagenesis of acidic residues in putative membrane-spanning segments of the melibiose permease of *Escherichia coli*. I. Effect on Na(+)-dependent transport and binding properties. *J Biol Chem.* 1993; 268:3209–3215. [PubMed: 8428997]
- (31). Hama H, Wilson TH. Replacement of alanine 58 by asparagine enables the melibiose carrier of *Klebsiella pneumoniae* to couple sugar transport to Na<sup>+</sup>. *J Biol Chem.* 1994; 269:1063–1067. [PubMed: 8288562]
- (32). Matsuzaki S, Weissborn AC, Tamai E, Tsuchiya T, Wilson TH. Melibiose carrier of *Escherichia coli*: use of cysteine mutagenesis to identify the amino acids on the hydrophilic face of transmembrane helix 2. *Biochim Biophys Acta.* 1999; 1420:63–72. [PubMed: 10446291]
- (33). Zani ML, Pourcher T, Leblanc G. Mutagenesis of acidic residues in putative membrane-spanning segments of the melibiose permease of *Escherichia coli*. II. Effect on cationic selectivity and coupling properties. *J Biol Chem.* 1993; 268:3216–3221. [PubMed: 8428998]
- (34). Zani ML, Pourcher T, Leblanc G. Mutation of polar and charged residues in the hydrophobic NH<sub>2</sub>-terminal domains of the melibiose permease of *Escherichia coli*. *J Biol Chem.* 1994; 269:24883–24889. [PubMed: 7929169]
- (35). Franco PJ, Wilson TH. Arg-52 in the melibiose carrier of *Escherichia coli* is important for cation-coupled sugar transport and participates in an intrahelical salt bridge. *J Bacteriol.* 1999; 181:6377–6386. [PubMed: 10515928]
- (36). Franco PJ, Jena AB, Wilson TH. Physiological evidence for an interaction between helices II and XI in the melibiose carrier of *Escherichia coli*. *Biochim Biophys Acta.* 2001; 1510:231–242. [PubMed: 11342161]
- (37). Hacksell I, Rigaud JL, Purhonen P, Pourcher T, Hebert H, Leblanc G. Projection structure at 8 Å resolution of the melibiose permease, an Na-sugar co-transporter from *Escherichia coli*. *EMBO J.* 2002; 21:3569–3574. [PubMed: 12110569]
- (38). Purhonen P, Lundback AK, Lemonnier R, Leblanc G, Hebert H. Three-dimensional structure of the sugar symporter melibiose permease from cryo-electron microscopy. *J Struct Biol.* 2005; 152:76–83. [PubMed: 16139519]
- (39). Huang Y, Lemieux MJ, Song J, Auer M, Wang DN. Structure and mechanism of the glycerol-3-phosphate transporter from *Escherichia coli*. *Science.* 2003; 301:616–620. [PubMed: 12893936]
- (40). Gouaux E, Mackinnon R. Principles of selective ion transport in channels and pumps. *Science.* 2005; 310:1461–1465. [PubMed: 16322449]
- (41). Oldham ML, Khare D, Quioco FA, Davidson AL, Chen J. Crystal structure of a catalytic intermediate of the maltose transporter. *Nature.* 2007; 450:515–521. [PubMed: 18033289]

- (42). Forrest LR, Zhang YW, Jacobs MT, Gesmonde J, Xie L, Honig BH, Rudnick G. Mechanism for alternating access in neurotransmitter transporters. *Proc Natl Acad Sci U S A*. 2008; 105:10338–10343. [PubMed: 18647834]
- (43). Law CJ, Maloney PC, Wang DN. Ins and outs of major facilitator superfamily antiporters. *Annu Rev Microbiol*. 2008; 62:289–305. [PubMed: 18537473]
- (44). Khare D, Oldham ML, Orelle C, Davidson AL, Chen J. Alternating access in maltose transporter mediated by rigid-body rotations. *Mol Cell*. 2009; 33:528–536. [PubMed: 19250913]
- (45). Abramson J, Wright EM. Structure and function of Na(+)-symporters with inverted repeats. *Curr Opin Struct Biol*. 2009; 19:425–432. [PubMed: 19631523]
- (46). Kaback HR, Smirnova I, Kasho V, Nie Y, Zhou Y. The alternating access transport mechanism in LacY. *J Membr Biol*. 2011; 239:85–93. [PubMed: 21161516]
- (47). Sixma TK, Pronk SE, Kalk KH, van Zanten BA, Berghuis AM, Hol WG. Lactose binding to heat-labile enterotoxin revealed by X-ray crystallography. *Nature*. 1992; 355:561–564. [PubMed: 1741035]
- (48). Duan X, Quioco FA. Structural evidence for a dominant role of nonpolar interactions in the binding of a transport/chemosensory receptor to its highly polar ligands. *Biochemistry*. 2002; 41:706–712. [PubMed: 11790091]
- (49). Guan L, Hu Y, Kaback HR. Aromatic stacking in the sugar binding site of the lactose permease. *Biochemistry*. 2003; 42:1377–1382. [PubMed: 12578349]
- (50). Faham S, Watanabe A, Besserer GM, Cascio D, Specht A, Hirayama BA, Wright EM, Abramson J. The crystal structure of a sodium galactose transporter reveals mechanistic insights into Na<sup>+</sup>/sugar symport. *Science*. 2008; 321:810–814. [PubMed: 18599740]
- (51). Cordat E, Leblanc G, Mus-Veteau I. Evidence for a role of helix IV in connecting cation- and sugar-binding sites of *Escherichia coli* melibiose permease. *Biochemistry*. 2000; 39:4493–4499. [PubMed: 10757998]
- (52). Wilson DM, Hama H, Wilson TH. GLY113-->ASP can restore activity to the ASP51-->SER mutant in the melibiose carrier of *Escherichia coli*. *Biochem Biophys Res Commun*. 1995; 209:242–249. [PubMed: 7726841]
- (53). Ganea C, Meyer-Lipp K, Lemonnier R, Krah A, Leblanc G, Fendler K. G117C MelB, a mutant melibiose permease with a changed conformational equilibrium. *Biochim Biophys Acta*. 2011; 1808:2508–2516. [PubMed: 21801712]
- (54). Kaback, HR. Bacterial Membranes. In: Kaplan, NP.; Jakoby, WB.; Colowick, NP., editors. *Methods in Enzymol*. Elsevier; New York: 1971. p. 99-120.
- (55). Short SA, Kaback HR, Kohn LD. D-lactate dehydrogenase binding in *Escherichia coli* dld-membrane vesicles reconstituted for active transport. *Proc Natl Acad Sci U S A*. 1974; 71:1461–1465. [PubMed: 4598306]
- (56). Niiya S, Moriyama Y, Futai M, Tsuchiya T. Cation coupling to melibiose transport in *Salmonella typhimurium*. *J Bacteriol*. 1980; 144:192–199. [PubMed: 6998948]
- (57). Cordat E, Mus-Veteau I, Leblanc G. Structural studies of the melibiose permease of *Escherichia coli* by fluorescence resonance energy transfer. II. Identification of the tryptophan residues acting as energy donors. *J Biol Chem*. 1998; 273:33198–33202. [PubMed: 9837888]
- (58). Carrasco N, Antes LM, Poonian MS, Kaback HR. lac permease of *Escherichia coli*: histidine-322 and glutamic acid-325 may be components of a charge-relay system. *Biochemistry*. 1986; 25:4486–4488. [PubMed: 2876725]
- (59). Guan L, Kaback HR. Lessons from lactose permease. *Annu Rev Biophys Biomol Struct*. 2006; 35:67–91. [PubMed: 16689628]
- (60). Bassilana M, Pourcher T, Leblanc G. Melibiose permease of *Escherichia coli*. Characteristics of co-substrates release during facilitated diffusion reactions. *J Biol Chem*. 1988; 263:9663–9667. [PubMed: 2838475]
- (61). Hama H, Wilson TH. Cation-coupling in chimeric melibiose carriers derived from *Escherichia coli* and *Klebsiella pneumoniae*. The amino-terminal portion is crucial for Na<sup>+</sup> recognition in melibiose transport. *J Biol Chem*. 1993; 268:10060–10065. [PubMed: 8387512]

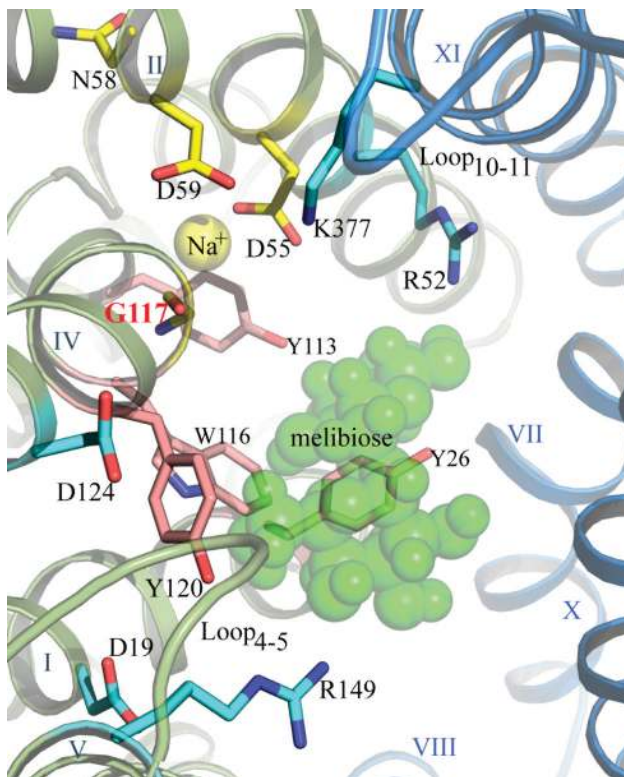


**Fig. 1.** Putative cosubstrate-binding sites of MelB viewed from the cytoplasmic side. The N- and C-terminal helix bundles are shown in green and blue, respectively. The residues essential (D55 and D59) or important (N58) for  $\text{Na}^+$  binding in MelB<sub>Ec</sub> are shown as yellow sticks. Residues colored in cyan (D19, D124, R52, R149, and K377) and pink (Y26, Y113, W116, and Y120) are important for melibiose binding/transport in MelB<sub>Ec</sub>. The Gly117 is shown by backbone (yellow) and labeled in red. Important loops between helices IV–V and X–XI are labeled as Loop<sub>4-5</sub> and Loop<sub>10-11</sub>, respectively. A melibiose molecule is shown in green.<sup>13</sup>

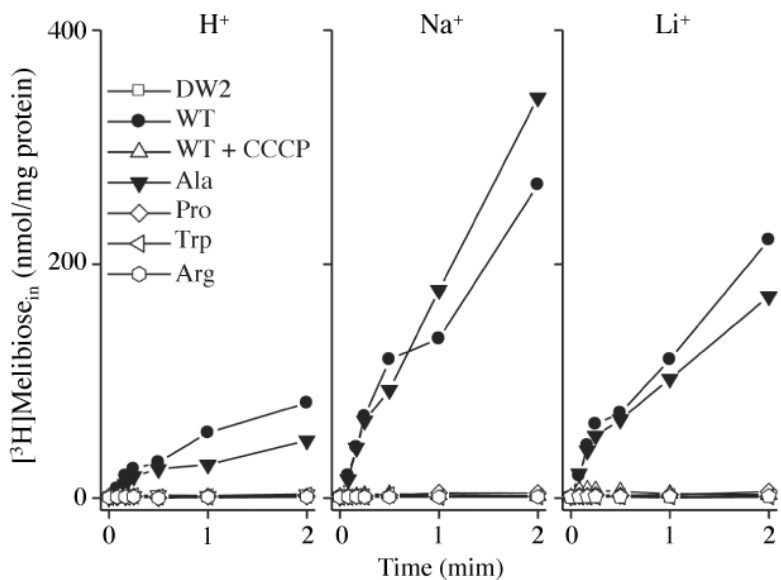


**Fig. 2.**

Melibiose transport in intact cells. *E. coli* DW2 cells were washed and resuspended with 100 mM  $KP_i$ , pH 7.5, 10 mM  $MgSO_4$ , and adjusted to 0.7 mg/ml of protein. Transport was initiated by adding melibiose (0.4 mM, 10 mCi/mmol) in the absence or presence of 20 mM NaCl or LiCl. Intracellular melibiose is plotted as a function of time. The cells expressing WT MelB<sub>St</sub> were treated with 10  $\mu$ M CCCP prior to the transport assay.



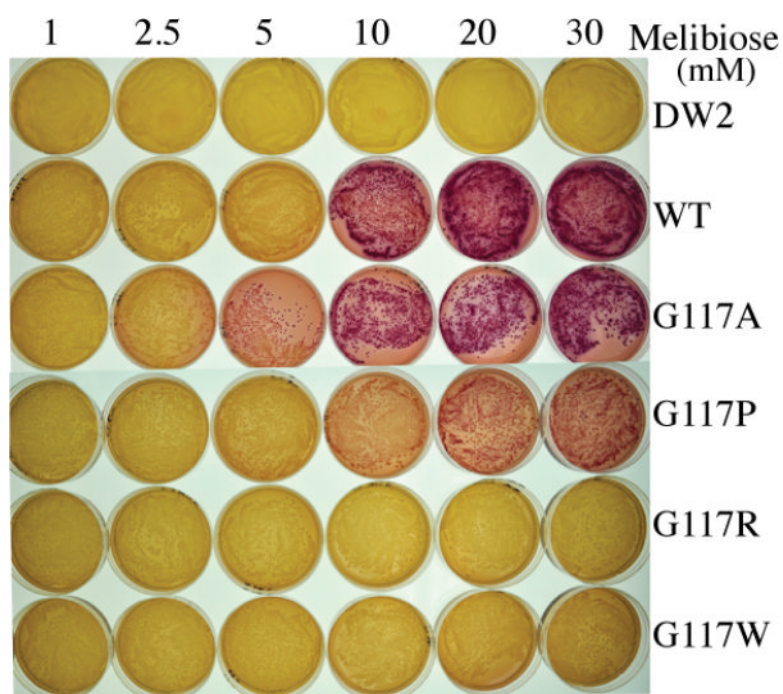


**Fig. 3.** Melibiose fermentation. *E. coli* DW2 (*lacY<sup>-</sup>Z melA<sup>+</sup>B<sup>-</sup>*) cells were transformed with a plasmid encoding the WT or a MelB<sub>S<sub>t</sub></sub> mutant, and plated on MacConkey agar (lactose free) containing concentrations of melibiose ranging from 1 mM to 30 mM, and incubated at 37 °C for 18 h.

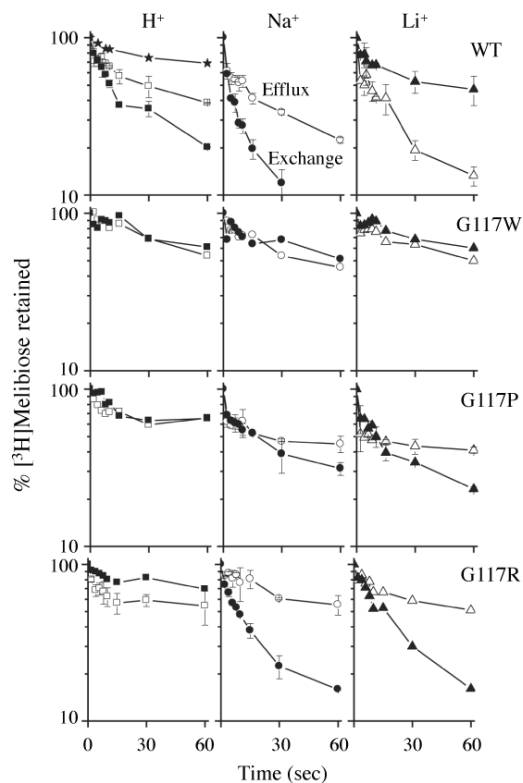


**Fig. 4.** Melibiose efflux and exchange. Melibiose efflux (open symbols) was measured by diluting the preloaded vesicles without (*squares*) or with 20 mM NaCl (*circles*) or LiCl (*triangles*) in a buffer containing 100 mM  $KP_i$ , pH 7.5, without or with 20 mM NaCl or LiCl, respectively. Melibiose exchange (*filled symbols*) was assessed in the same way except for the presence of 20 mM unlabeled melibiose in the dilution buffer. For a negative control, RSO vesicles containing WT MelB<sub>St</sub> were treated with 3.6 mM 2-(4'-maleimidylanilino)-naphthalene-6-sulfonic acid for 5 hr at 23 °C (*stars*), and diluted into 100 mM  $KP_i$ , pH 7.5 in the absence of melibiose.<sup>1</sup> Intracellular melibiose was expressed as a percentage of the zero-time point. Error bars indicate S.D.

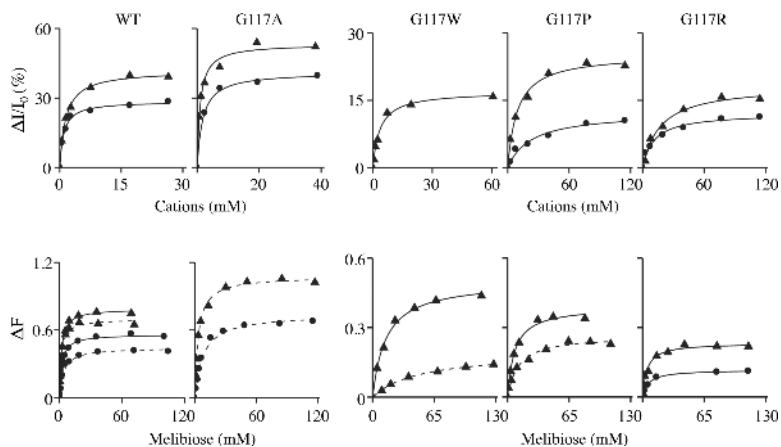


**Fig. 5.** Apparent affinity. RSO vesicles (0.5 mg/ml, 100 mM  $KP_i$ , pH 7.5) containing WT or a MelB<sub>St</sub> mutant were used for D<sup>2</sup>G FRET assay at excitation and emission wavelengths of 290 and 500 nm, respectively. (*Top panels*): Determination of  $K_{0.5}^{Na^+}$  and  $K_{0.5}^{Li^+}$  for the D<sup>2</sup> 0.5 G FRET. With 10  $\mu$ M D<sup>2</sup>G, Na<sup>+</sup> or Li<sup>+</sup> was added at increasing concentrations. The normalized emissions were plotted as a function of Na<sup>+</sup> (circles) or Li<sup>+</sup> (triangles) concentration.  $K_{0.5}^{Na^+}$  or  $K_{0.5}^{Li^+}$  value was determined by fitting a hyperbolic function to the data. (*Bottom panels*): Determination of IC<sub>50</sub> for melibiose displacement of bound D<sup>2</sup>G. With D<sup>2</sup>G (10  $\mu$ M) and Na<sup>+</sup> or Li<sup>+</sup> at a given concentration, melibiose were added stepwise until the displacement of the bound D<sup>2</sup>G is complete. After correction for the water dilution effect, the change in intensity ( $\Delta F$ ) was plotted as a function of melibiose concentration. The IC<sub>50</sub> value was determined by fitting a hyperbolic function to the data obtained in the presence of 20 mM Na<sup>+</sup> (circles with dashed lines), 200 mM Na<sup>+</sup> (circles with solid lines), 20 mM Li<sup>+</sup> (triangles with dashed lines), or 200 mM Li<sup>+</sup> (triangles with solid lines).

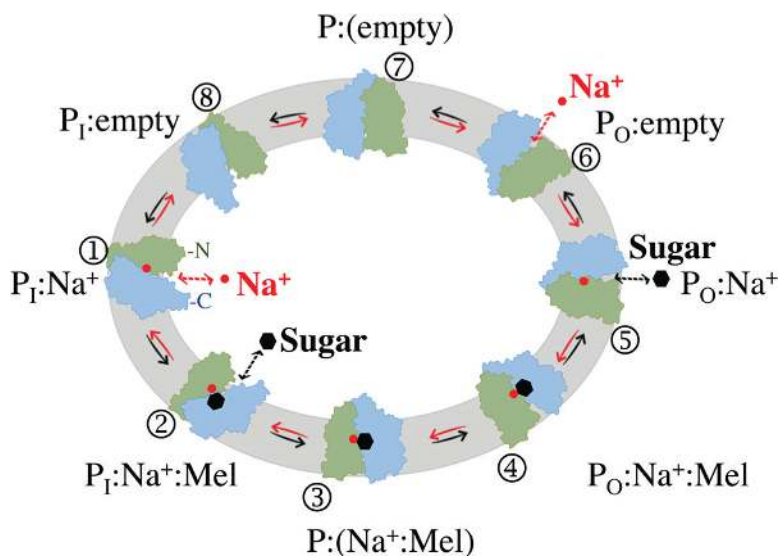


**Fig. 6.** An ordered-binding model for melibiose/ $\text{Na}^+$  efflux catalyzed by  $\text{MelB}_{\text{St}}$  (see text). The N- and C-terminal domains of  $\text{MelB}_{\text{St}}$  molecule are colored in green and blue, respectively. Sugar and  $\text{Na}^+$  are shown as black hexagons and red spheres, respectively.  $\text{P}_I$  or  $\text{P}_O$  represents the permease at an inward-facing or outward-facing conformation, respectively.  $\text{P}:(\text{Na}^+:\text{Mel})$  or  $\text{P}:(\text{empty})$ , cosubstrates-bound or unloaded permease at the occluded state, respectively.

Table 1

Cation stimulation constants for D<sup>2</sup>G FRET ( $K_{0.5}^{\text{Na+ or Li+}}$ , mM)

	WT	G117A	G117W	G117P	G117R
Na <sup>+</sup>	0.9	1.7	<sup>a</sup>	23.2	11.2
Li <sup>+</sup>	1.5	0.97	3.6	9.5	17.2

<sup>a</sup> not determined due to weak signals.



Table 2

IC<sub>50</sub> for melibiose displacement of bound D<sup>2</sup>-G (mM)

	WT	G117A	G117W	G117P	G117R
Na <sup>+</sup> 20 mM	3.8	8.1	<sup>a</sup>	/	/
200 mM	2.2	<sup>b</sup>	/	/	5.6
Li <sup>+</sup> 20 mM	1.7	3.4	50.0	11.3	/
200 mM	1.8	-	14.1	7.5	4.7

<sup>a</sup> not determined due to weak signals.

<sup>b</sup> not determined